X-Ray Diffraction and Calorimetric Study of N-Lignoceryl Sphingomyelin Membranes

Prakas R. Maulik and G. Graham Shipley
Departments of Biophysics and Biochemistry, Center for Advanced Biomedical Research, Boston University School of Medicine, Boston, Massachusetts 02118 USA

ABSTRACT Differential scanning calorimetry and x-ray diffraction have been used to investigate hydrated multibilayers of N-lignoceryl sphingomyelin (C24:0-SM) in the hydration range 0–75 wt % H_2O. Anhydrous C24:0-SM exhibits a single endothermic transition at 81.3°C (ΔH = 3.6 kcal/mol). At low hydration (12.1 wt % H_2O), three different endothermic transitions are observed: low-temperature transition (T_1) at 39.4°C (transition enthalpy (ΔH_1) = 2.8 kcal/mol), intermediate-temperature transition (T_2) at 45.5°C, and high-temperature transition (T_3) at 51.3°C (combined transition enthalpy (ΔH_{2+3}) = 5.03 kcal/mol). On increasing hydration, all three transition temperatures of C24:0-SM decrease slightly to reach limiting values of 36.7°C (T_1), 44.4°C (T_2), and 48.4°C (T_3) at ~20 wt % H_2O. At 22°C (below T_1), x-ray diffraction of C24:0-SM at different hydration levels shows two wide-angle reflections, a sharp one at 1/4.2 $Å^{-1}$ and a more diffuse one at 1/4.0 $Å^{-1}$ together with lamellar reflections corresponding to bilayer periodicities increasing from d = 65.4 Å to a limiting value of 71.1 Å. Electron density profiles show a constant bilayer thickness $d_{p\text{-}p}$ ~50 Å. In contrast, at 40°C (between T_1 and T_2) a single sharp wide-angle reflection at ~1/4.2 $Å^{-1}$ is observed. The lamellar reflections correspond to a larger bilayer periodicity (increasing from d = 69.3–80.2 Å) and there is some increase in $d_{p\text{-}p}$ (52–56 Å) with hydration. These structural parameters, together with calculated lipid thickness and molecular area considerations, suggest that the low temperature endotherm (T_1) of hydrated C24:0-SM corresponds to a transition from a tilted, gel state (Gel I) with partially interdigitated chains to an untilted, or less tilted, gel state (Gel II). At 60°C (above T_3), the usual liquid-crystalline L_α bilayer structure (d = 59.5–66.3 Å; $d_{p\text{-}p}$ ~46 Å) is present at all hydrations. Comparison with the behavior of C18:0-SM indicates that the inequivalence of length of the sphingosine (C18) and lignoceryl (C24) chains results in a more complex gel phase polymorphism for C24:0-SM.

INTRODUCTION

The basic structural motif of biological membranes is the lipid bilayer. The lipid bilayer provides both a general permeability barrier and a matrix into which membrane proteins are asymmetrically incorporated to fulfill their specific receptor, signaling, enzymatic, and channel functions. The bilayer compartment of mammalian membranes is composed of various classes of lipids, mainly phospholipids (e.g., phosphatidylcholine (PC), phosphatidylethanolamine, phosphatidylserine, phosphatidylinositol) and glycosphingolipids (e.g., cerebrosides, gangliosides), and cholesterol. Sphingomyelin (SM), a phosphosphingolipid with the phosphorylcholine polar group identical to that of PC, is also present in many membranes. Both SM and PC seem to favor a location at the outward facing monolayer of the membranes of erythrocytes and other cells; in addition, SM, PC, and cholesterol are the predominant polar lipids stabilizing the monolayer surface of the plasma lipoproteins, high density and low density lipoproteins, etc.

Apart from their ability to form phospholipid bilayers (and perhaps other structures), it is now becoming clear that several membrane lipids have a more specific functional role. For example, gangliosides seem to play a role in both cell-cell recognition events and as receptors for the binding of hormones, viruses, and toxins (Hakomori, 1981; Fishman et al., 1993). In addition, phosphatidylinositol and PC act as precursors of second messengers and intermediates (diacylglycerol, inositol triphosphate, arachidonic acid) in cell signaling pathways after receptor-mediated triggering of membrane phospholipases. Recently it was shown that SM is converted to ceramide after the removal of its phosphorylcholine head group by sphingomyelinase, again after ligand binding to membrane receptors. The released ceramide acts as a second messenger and seems to stimulate both protein kinase and protein phosphatase pathways, which in turn may regulate both cell growth and apoptosis (for recent reviews see Hannun, 1994, and Hannun and Obeid, 1995). Given the functional importance of SM and ceramide, studies on the structure and properties of these lipids would seem to be important.

In the past, we and many others have systematically studied the structural behavior of different phospholipid classes, and then for a specific phospholipid class have examined the effects of changes in hydrocarbon chain length, unsaturation, distribution, and linkage. This approach has led to a broad understanding of the phase behavior of phospholipids and the alterations in behavior produced by modifications to the polar group, chain, and interfacial regions. We have adopted a similar approach to the study of the properties of SM.

Received for publication 20 March 1995 and in final form 6 July 1995.

Address reprint requests to Dr. G. Graham Shipley, Department of Biophysics, Boston University School of Medicine, 80 E. Concord Street, Boston, MA 02118-2394. Tel.: 617-638-4009; Fax: 617-638-4041; E-mail: shipley@med-biophi.bu.edu.

0006-3495/95/11/1909/00 $2.00

Naturally occurring SMs are chemically heterogeneous. Although the sphingosine chain is predominantly C18:1 (*trans* Δ4–5), small amounts of the C20:1 and the dihydro- (sphinganine) analogs are present (Sripada et al., 1987). The amide-linked fatty acids include palmitic (C16:0) and stearic (C18:0) as well as the longer chain behenic (C22:0), lignoceric (C24:0), and nervonic (C24:1) acids (Calhoun and Shipley, 1979a). Our initial study of SM isolated from bovine brain showed that it exclusively formed bilayer phases but that its bilayer gel-liquid crystal transition occurred at an unusually high temperature (30–40°C) for a natural lipid, presumably due to the preponderance of saturated fatty acid chains (Shipley et al., 1974; see also Barenholz et al., 1976). The complexity arising from the chemical heterogeneity of natural SM has been addressed using two synthetic approaches. First, starting with natural SM, the fatty acid heterogeneity can be removed by deacylation-reacylation partial synthetic protocols (Ahmad et al., 1985; Cohen et al., 1984); however, heterogeneity associated with the sphingosine moiety is left in place. Alternatively, methods for the de novo synthesis of SM are now becoming available (Shapiro, 1969; Bruzik, 1988; Dong and Butcher, 1993).

We have synthesized a series of N-acyl SM containing C14:0, C16:0, C18:0, C20:0, C22:0, and C24:0 fatty acids by deacylation-reacylation of bovine brain SM (Sripada et al., 1987). Initial calorimetric studies showed that C16:0-, C18:0-, and C20:0-SM exhibit simple, reversible chain-melting transitions, whereas the short chain (C14:0) and long chain (C22:0 and C24:0) SM exhibit more complex thermotropic behavior with multiple transitions, presumably due to a mismatch in the length of the N-acyl chain compared with the sphingosine chain (Sripada et al., 1987). This mismatch would be expected to cause packing problems in the bilayer gel state, but our x-ray scattering studies of this series of SMs suggest that bilayer packing perturbations due to chain interdigitation effects also occur in the liquid crystalline state, at least in single bilayer vesicles (Maulik et al., 1986a).

Calorimetric and x-ray diffraction studies of members of the above series have been reported. Fully hydrated C16:0- and C18:0-SM exhibit simple thermotropic behavior with reversible transitions at 40.5 and 45.0°C, respectively, between bilayer gel and liquid crystalline phases (Maulik et al., 1991; Maulik et al., 1986b). For stereochemically pure D-erythro- and L-threo-C18:0-SM, Bruzik and Tsai (1987) observed similar transitions and also showed that appropriate incubation protocols lead to the formation of additional gel phases. More recently, the properties of the longer chain, more asymmetric SM have been addressed. For example, McIntosh et al. (1992a) described the properties of fully hydrated C24:0-SM and its interaction with equimolar cholesterol and then defined the interbilayer interactions of these two bilayer systems (McIntosh et al., 1992b). Our own studies of N-lignoceryl-SM (C24:0-SM) reported here focus on its hydration dependence, with particular emphasis on the structures of the various gel and liquid crystalline phases that were formed.

MATERIALS AND METHODS

C24:0-SM

C24:0-SM was prepared by partial synthesis from bovine brain SM (Calbiochem-Boehring Diagnostic, San Diego, CA) after acid hydrolysis deacylation to sphingosylphosphorylcholine (SPC) followed by reacylation of SPC using fatty acyl imidazoles (Sripada et al., 1987). The C24:0-SM was shown to be >99% pure by a combination of thin layer chromatography and high performance liquid chromatography; however, as noted previously (Sripada et al., 1987; Maulik et al., 1991), epimerization at C-3 of sphingosine does occur during the acid hydrolysis step, leading to the formation of some of the L-threo stereoisomer of SPC. Because we have been unable to separate the stereoisomers of either SPC or the reacylated SM, the desired product, D-erythro-SM, does contain ~25% of the L-threo isomer (for a detailed discussion of this issue for C16:0-SM, see Sripada et al., 1987). For the starting material, bovine brain SM, the predominant sphingosine base is C18:1t (90.2%) plus minor amounts of C20:1t (7.3%) and C18:0 (2.6%). In our detailed study of C16:0-SM (Sripada et al., 1987), C18:1t is retained as the major sphingosine base (85.7%), with changes occurring in the levels of the minor sphingosine components. A similar sphingosine profile is to be expected for C24:0-SM, with C18:1t the predominant (~90%) molecular species.

Differential scanning calorimetry (DSC)

For DSC studies, anhydrous samples were weighed into stainless steel pans, and the calculated amount of deionized, double-distilled water was added using a Hamilton syringe to give various hydration states of C24:0-SM. The sample pans were hermetically sealed and then placed in a Perkin-Elmer DSC-2 differential scanning calorimeter (Norwalk, CT) equipped with a thermal analysis data station. Sample equilibration was achieved by successive heating/cooling cycles over the temperature range 0–88°C. Heating and cooling scans of the samples were performed in the temperature range 0–100°C at heating/cooling rates of 5°C/min. The transition enthalpies (ΔH) were determined from the area under the peaks of the recorded heat capacity versus temperature plots, after calibration with a gallium standard.

X-ray diffraction

For x-ray diffraction, samples of anhydrous C24:0-SM were weighed directly into thin-walled glass or quartz capillaries (internal diameter = 1.0 mm) and appropriate amounts of deionized, double-distilled water were added using a Hamilton syringe. The capillary tubes were immediately flame-sealed, followed by epoxy coating at the seal to eliminate leaks. The capillaries were centrifuged, inverted, and recentrifuged several times at temperatures 10°C above the chain-melting temperature (with intermittent cooling to room temperature) to achieve equilibration of the multilamellar lipid/water systems.

The x-ray diffraction patterns of equilibrated C24:0-SM at different hydrations were recorded on photographic film using focusing cameras with either toroidal mirror (Elliott, 1965) or double-mirror (Franks, 1958) optics. Nickel-filtered CuK_α (λ = 1.5418 Å) radiation was obtained from an Elliot GX6 rotating anode generator (Elliot Automation, Borehamwood, UK). Diffraction patterns were recorded initially at 22°C, then at 40–43°C depending on the hydration (see Results section), and finally at 60°C. Samples were kept at constant temperature using a circulating ethylene glycol/water bath. The relative intensities of the diffraction lines were measured using a Joyce-Loebl (Gateshead, UK) Model IIICS scanning microdensitometer.

Bilayer periodicities, d, at each hydration were calculated from the lamellar reflections using Bragg's law ($2d \sin \theta = n\lambda$). Starting with the bilayer periodicity, values for lipid bilayer thickness (d_l) and surface

area per SM molecule at the lipid/water interface (S) were calculated at different lipid concentrations according to the formalism of Luzzati (1968). For these calculations, the partial specific volumes (V_l) for C24:0-SM were assumed to be 0.955 ml/g at 22°C, 0.971 ml/g at 40°C (0.974 ml/g at 43°C and 0.972 at 41°C), and 1.045 ml/g at 60°C (corresponding to values for similar phases of the structurally related distearoyl-PC; Nagle and Wilkinson, 1978). The molecular weight of C24:0-SM was 815.3.

To calculate electron density profiles, the observed intensities of the lamellar low angle reflections were corrected for the Lorentz factors, scaled, normalized, and converted to structure amplitudes F_s (Worthington and Blaurock, 1969). Phases of the lamellar reflections were determined by inspection of the plotted structure amplitudes as a function of the reciprocal coordinate s (s = 2 sin θ/λ) (Torbet and Wilkins, 1976; Janiak et al., 1979; McIntosh and Simon, 1986) and by the use of the Shannon sampling theorem (Shannon, 1949; King and Worthington, 1971).

RESULTS

DSC of C24:0-SM

DSC heating/cooling scans of C24:0-SM at different hydration levels were performed over the temperature ranges 0–88°C (for hydrated samples) and 0–100°C (for anhydrous samples) at heating/cooling rates of 5°C/min. Fig. 1 shows representative DSC heating scans corresponding to the third heating run (after initial and second heating/cooling cycles) of C24:0-SM in the hydration range 0–74.8 wt % water. Corresponding cooling scans at 5°C/min reveal essentially reversible behavior at all hydrations, the same multiple transitions (with little or no supercooling) being observed. Although the initial heating/cooling scans occasionally showed evidence of sample inequilibration, all successive heating/cooling scans were essentially identical and reversible, indicating complete sample equilibration. In the absence of water, C24:0-SM exhibits a sharp endothermic transition (with a low temperature shoulder) at 81.3°C (ΔH = 3.6 kcal/mol). Highly hydrated (74.8 wt %) C24:0-SM exhibits more complex behavior, with a low-temperature transition at 34.9°C (ΔH = 3.0 kcal/mol) and a high-temperature transition at 44.2°C (ΔH = 6.1 kcal/mol) with a shoulder at ~48°C. At low hydration (12.1 wt % H_2O), C24:0-SM exhibits three clearly distinct endothermic transitions (Fig. 1): a low-temperature transition (T_1) at 39.4°C, an intermediate-temperature transition (T_2) at 45.5°C, and a high-temperature transition (T_3) at 51.3°C. The ΔH of T_1 is 2.8 kcal/mol, and the combined enthalpy (ΔH_{2+3}) associated with T_2 and T_3 is 5.0 kcal/mol. As the hydration increases over the range 12.1–31.6 wt %, T_1 decreases to 36.7°C, T_2 to 44.4°C, and T_3 to 48.4°C. When more water is added, no significant changes in transition temperatures occur, but the third transition (T_3) becomes significantly broader at the higher hydrations (see Fig. 1). The enthalpy (ΔH_1) associated with T_1 remains almost constant at all hydration levels, whereas the enthalpy (ΔH_{2+3}) associated with T_2 and T_3 increases slightly with increasing hydration, reaching a limiting value of 5.7 kcal/mol at 30.6 wt % water. Plots of transition temperatures (T_1, T_2, and T_3) and ΔH_1 and ΔH_{2+3} of C24:0-SM are shown as a function of water content in Fig. 2, *a* and *b*, respectively.

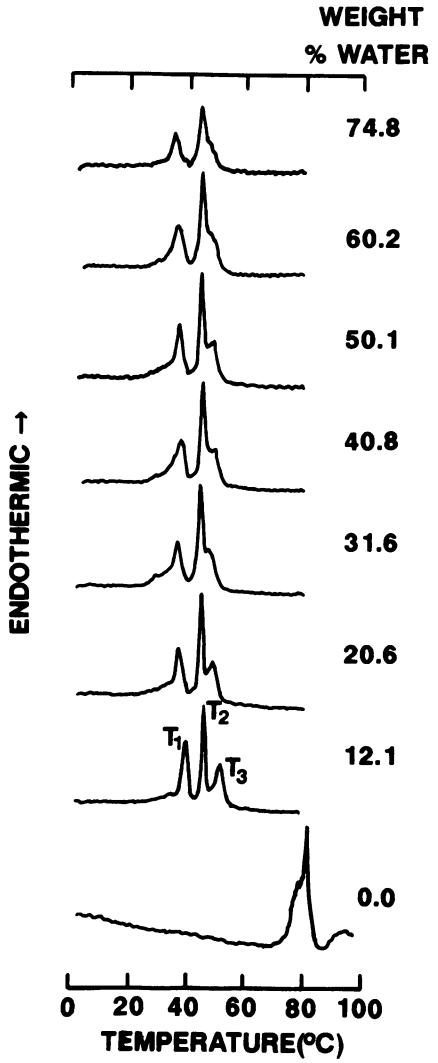

FIGURE 1 Representative DSC heating scans of hydrated C24:0-SM in the range 0.0–74.8 wt % water. Heating rates: 5°C/min. The third heating scan following two heating/cooling (5°C/min) cycles is shown.

X-ray diffraction of hydrated C24:0-SM

X-ray diffraction data were recorded at 22°C, 40°C, and 60°C from hydrated (9.1–35.2 wt % H_2O) C24:0-SM. At lower hydrations, diffraction patterns were also recorded at 43°C for 9.1 wt % H_2O and at 41°C for 14.2 wt % H_2O. Because of increasing overlap of T_2 and T_3 with hydration, we were unable to study the structure that was present between these two phase transitions. As an example, for 19.6 wt % below T_1 at 22°C, a series of lamellar low-angle reflections (orders h = 1 → 8; h = 7, 8 are weak) are observed corresponding to a bilayer periodicity, d = 70.1 Å. The wide-angle region shows a sharp reflection at 1/4.18 $Å^{-1}$ and a broad shoulder at 1/3.99 $Å^{-1}$. This diffraction pattern is typical of that observed for hydrated phospholipid bilayers in the gel phase (Gel I), with tilted hydrocarbon chains and pseudohexagonal chain packing (Tardieu et al., 1973; Ruocco and Shipley, 1982; Wiener et al., 1989). On

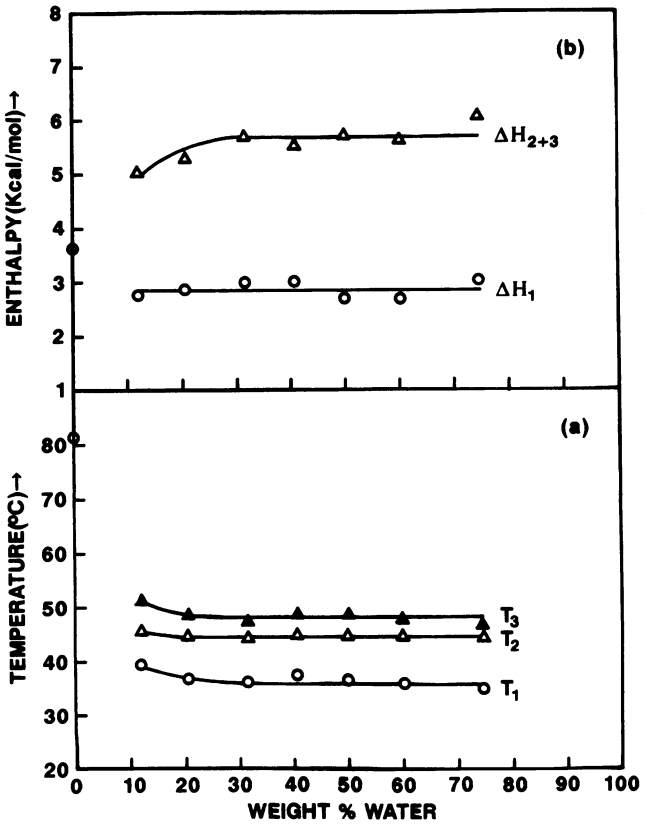

FIGURE 2 (*a*) Transition temperatures and (*b*) transition enthalpies of C24:0-SM as a function of hydration (wt % water). In (*a*), the transitions are indicated as follows: (○) low temperature transition (T_1); (△), intermediate transition (T_2); (▲), high temperature transition (T_3). In (*b*), (○), enthalpy (ΔH_1) associated with T_1 and (△) combined enthalpy (ΔH_{2+3}) associated with T_2 and T_3 are indicated.

heating to 40°C, corresponding to a temperature between T_1 and T_2, the diffraction pattern shows lamellar low-angle reflections ($h = 1 \rightarrow 6$; $h = 5,6$ are weak) corresponding to a slightly increased bilayer periodicity, $d = 72.7$ Å, and a single sharp wide-angle reflection at 1/4.22 Å, indicating that in this bilayer gel phase (Gel II) the hydrocarbon chains are packed in a hexagonal lattice without chain tilting. At 60°C, above T_3, a series of lamellar low-angle reflections ($h = 1 \rightarrow 6$) is again observed but corresponding to a reduced bilayer periodicity, $d = 60.4$ Å. The broad, diffuse diffraction line in the wide-angle region at 1/4.6 $Å^{-1}$ is characteristic of the melted-chain liquid-crystalline L_α phase. At these temperatures (22, 40, and 60°C), similar lamellar x-ray diffraction patterns were observed for C24:0-SM at other hydration levels (see below).

From the measured bilayer periodicity and the compositional parameters (see Materials and Methods section), the bilayer thickness (d_l) and the mean molecular surface area of the C24:0-SM molecule at the lipid/water interface, S, were calculated at 22°C (Gel I phase), 40°C (Gel II phase), and 60°C (L_α phase) at different hydrations (Luzzati, 1968). These calculated structural parameters (d_l and S) and the bilayer periodicity are plotted as a function of hydration at 22, 40 and 60°C in Fig. 3, *a–c*, respectively.

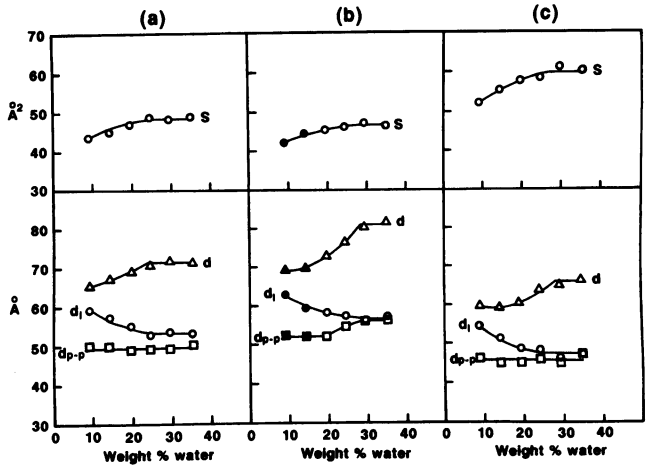

FIGURE 3 Bilayer structural parameters of C24:0-SM as a function of water content at (*a*) 22°C, (*b*) 40°C, and (*c*) 60°C. In the lower plots, (△) lamellar repeat distance, d; (○) lipid thickness d_l; and (□) phosphate-phosphate distance, $d_{p\text{-}p}$ are indicated. In the upper plots, (○) surface area per C24:0-SM molecule at the lipid/water interface, S, is indicated. In (*b*), the full symbols ● (*upper*) and ▲, ●, ■ (*lower*) represent S, d, d_l, and $d_{p\text{-}p}$, respectively, at 43°C for 9.1 wt % water and 41°C for 14.2 wt % water (see text).

At 22°C, C24:0-SM bilayers swell over the hydration range 9.1–24.5 wt % H_2O, the bilayer periodicity increasing from 65.4 to 71.1 Å; no further change in the bilayer periodicity is observed at >24.5 wt % H_2O, thus defining the hydration limit of the Gel I phase of C24:0-SM (Fig. 3 *a*). The calculated lipid thickness decreases from $d_l = 59.2$ Å at 9.1 wt % H_2O until a limiting value of $d_l = 52.9$ Å is reached at 25 wt % H_2O; the calculated surface area per C24:0-SM molecule (S) increases over the same hydration range from 43.7 $Å^2$ to a limiting value of 48.9 $Å^2$. At 40°C (43°C for 9.1 wt % H_2O and 41°C for 14.2 wt % H_2O), C24:0-SM exhibits a bilayer Gel II phase at all hydrations. The bilayer periodicity increases from $d = 69.3$ Å at 9.1 wt % H_2O, reaching a limiting value $d = 80.2$ Å at 30 wt % H_2O (Fig. 3 *b*). Over the hydration range 9.1–29.5 wt % H_2O, d_l decreases from 62.8 Å to 55.9 Å, and S increases from 42.0 $Å^2$ to 47.0 $Å^2$. At 60°C, over the hydration range 9.1–29.5 wt % H_2O, the liquid crystal bilayer phase of C24:0-SM exhibits bilayer swelling, with d increasing from 59.5 Å to 66.3 Å (Fig. 3c). For water contents >29.5 wt % H_2O, no further swelling is observed; d_l decreases from 54.3 Å at 9.1 wt % H_2O to a limiting value of 48.4 Å at 29.5 wt % H_2O, and S increases from 52.1 $Å^2$ to a limiting value of 61.3 $Å^2$ over the same hydration range.

In order to further define the C24:0-SM bilayer structure, electron density profiles across the SM bilayer have been calculated at different hydrations. Phasing of the bilayer structure amplitudes was achieved using the swelling method. The swelling experiments performed at 22, 40, and 60°C provide structure amplitudes F_s for the three bilayer phases (Gel I, Gel II, and L_α). The normalized amplitudes are plotted as a function of reciprocal space coordinate s ($s = 2 \sin \theta/\lambda$) for all hydrations as shown in Fig. 4, in order to trace the continuous transform (the amplitude curve of

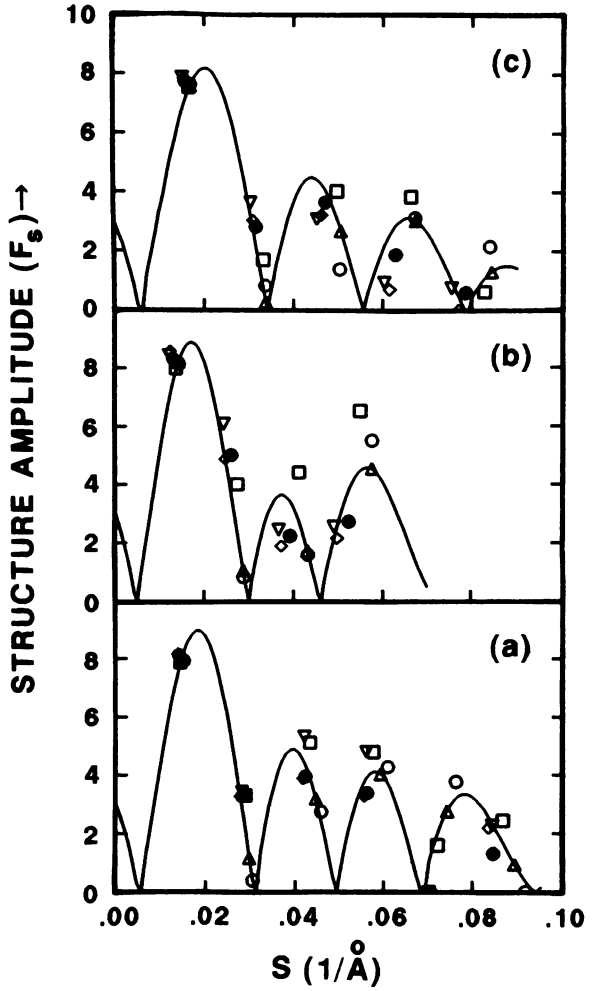

FIGURE 4 Structure amplitudes F_s of C24:0-SM bilayers at different hydrations: (*a*) 22°C, (*b*) 40°C (41°C at 9.1 wt % water and 43°C at 14.2 wt % water), and (*c*) 60°C. (○) 9.1 wt % water; (△) 14.2 wt % water; (□) 19.6 wt % water; (●) 24.5 wt % water; (◇) 29.5 wt % water; (▽) 35.2 wt % water. Continuous curves are derived by application of the Shannon sampling theorem for the data of C24:0-SM at 14.2 wt % water.

the bilayer profile) from which the phases of the structure amplitudes can be determined. The nodes, i.e., the points at which a phase change probably occurs, are identified by inspection to determine the signs of the structure amplitudes. The solid curves (Fig. 4) are calculated by the Shannon sampling theorem using the amplitude data of C24:0-SM at 14% hydration. Thus, the phase sequences −, −, +, −, +, + (22°C; Fig. 4 *a*); −, −, +, − (40°C; Fig. 4 *b*); and −, −, +, −, + (60°C; Fig. 4 *c*) were deduced, and the electron density profiles $\rho(x)$ calculated on the basis of these phases are shown in Fig. 5. At 22°C (Fig. 5 *a*) the centrosymmetric profiles at all hydrations are typical of a "bilayer" structure, with two symmetry-related peaks at 24.5–25.0 Å enclosing a region of lower electron density. These profiles closely resemble those reported by McIntosh et al. (1992a,b) for C24:0-SM. It should be noted that the shape of the profiles at the bilayer center differs somewhat from the pronounced trough observed for other gel phases.

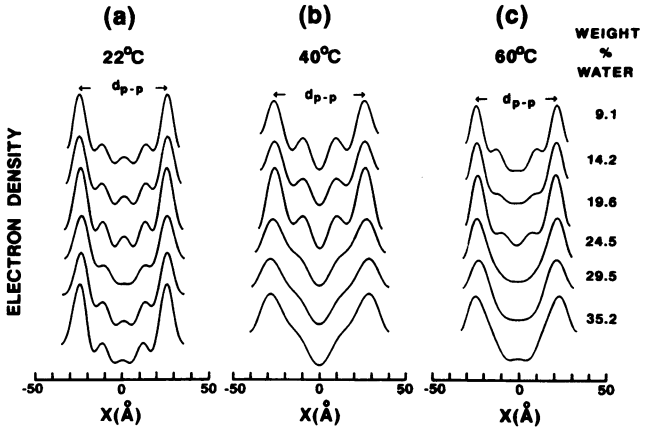

FIGURE 5 Electron density profiles, $\rho(x)$ for C24:0-SM at different hydrations: (*a*) 22°C, (*b*) 40°C (43/41°C for 9.1 and 14.2 wt % water), and (*c*) 60°C. Arbitrary scale.

The two peaks are due to the electron-rich phosphate groups of the polar moiety of C24:0-SM, and their separation across the bilayer (d_{p-p}) provides an additional measure of the bilayer thickness. The interlayer peak separation (not shown in Fig. 5) provides a measure of the water layer thickness, $d_w = d\text{-}d_{p-p}$.

Similar bilayer characteristics in the electron density profiles of C24:0-SM for all hydration levels are also observed at 40°C (Fig. 5 *b*) and at 60°C (Fig. 5 *c*), although compared with Fig. 5 *a*, the profiles are less detailed at the bilayer center. Also, the profiles in general become less detailed as the hydration increases and the resolution decreases. Values of d_{p-p} are plotted as a function of hydration at 22, 40, and 60°C in the lower panels of Fig. 3 *a–c*, respectively. Inspection of Fig. 5, *a* and *c* (see also Fig. 3, *a* and *c*) shows that the bilayer thickness is essentially independent of hydration, with d_{p-p} constant at 49–50 Å in the Gel I phase (22°C) and at 45–47 Å in the liquid crystal L_α phase (60°C). The water layer thickness, d_w, increases from 15.4 Å (9.1 wt % H_2O) to 21.9 Å (24.5 wt % H_2O) in the Gel I phase and from 13.5 Å (9.1 wt % H_2O) to 20.0 Å (29.5 wt % H_2O) in the L_α phase (data not shown).

In the Gel II phase at 40°C (Figs. 3 *b* and 5 *b*), d_{p-p} (= 52 Å) is constant at lower hydration levels (over the range 9.1–19.6 wt % H_2O). On increasing hydration, d_{p-p} apparently increases to 56 Å at hydration levels >29.5 wt % H_2O. The water layer thickness, d_w, increases from 17.3 Å to 25.5 Å on increasing hydration over the entire hydration range (data not shown).

DISCUSSION

Studies of phospholipids, glycolipids, and glycosphingolipids differing in chain length, unsaturation, distribution, etc., have revealed a myriad of different structures and structural interconversions. The different structures found in the chain-melted liquid crystalline phase include bilayer (L_α), hexagonal, cubic, and micellar phases. In contrast, the or-

dered chain gel or crystalline phases seem to be built exclusively on the bilayer geometry with the structural variety provided by differences in chain packing, chain order, chain tilt, chain interdigitation, and presumably in some cases, head group conformation and packing. Structural studies, particularly of PCs, have shown that under certain conditions PCs can adopt a fully interdigitated "monolayer" type of bilayer structure (Ranck et al., 1977; Serrallach et al., 1983; McDaniel et al., 1983; Simon and McIntosh, 1984; Braganza and Worcester, 1986; Ruocco et al., 1985; Kim et al., 1987; Haas et al., 1990). Mixed chain PCs in which one chain (at the *sn*-1 or *sn*-2 position) is systematically reduced show progressive interdigitation of the two chains across the bilayer center with presumably a longer chain juxtaposed against a shorter chain from the opposite monolayer (see Fig. 6 in Mattai et al., 1987). Furthermore, PCs in which the length of one of its constituent chains is approximately half the length of the other seem to pack in a "mixed interdigitated" monolayer structure, in this case with the two short chains from PC molecules on each side of the bilayer being aligned against each other and the hydrocarbon width essentially being determined by the long chain (Mattai et al., 1987; McIntosh et al., 1984; Hui et al., 1984; Shah et al., 1990).

In contrast to the structural studies of mixed-chain PCs, relatively little is known about the structure and properties of SM containing hydrocarbon (sphingosine and N-acyl) chains of different length. Our first DSC studies showed clearly that the highly asymmetric C24:0-SM exhibited two or three transitions suggestive of gel phase polymorphism (Sripada et al., 1987). Spectroscopic studies of synthetic DL-erythro C24:0-SM provided evidence for the presence of both mixed chain and partially interdigitated gel state bilayer structures below the chain-melting transition (Levin et al., 1985). Our x-ray scattering study of SM vesicles suggested that progressive chain interdigitation occurred across the bilayer center as the N-linked fatty acyl chain length increased up to C-24 with respect to the invariant C-18 sphingosine chain (Maulik et al., 1986a). More recently, McIntosh et al. (1992a), using x-ray diffraction, showed that hydrated C24:0-SM at 20°C adopts a partially interdigitated structure and that addition of cholesterol reduces the chain interdigitation. Here we focus on the structural changes exhibited by C24:0-SM as a function of hydration and temperature.

Our DSC data (Figs. 1 and 2) show that the thermotropic behavior of hydrated C24:0-SM differs markedly from that of SMs containing shorter N-linked acyl chains (for example, C16:0- and C18:0-SM). In contrast to the simple, reversible chain-melting transitions of C16:0- and C18:0-SM (Sripada et al., 1987; Maulik et al., 1991; Maulik et al., 1986b), C24:0-SM exhibits relatively complex thermotropic properties. Highly hydrated (74.8 wt % H_2O) C24:0-SM shows two transitions, T_1 at 34.9°C and T_2 at 44.2°C, the latter having a high temperature shoulder at ~48°C. Thermotropic behavior involving two endothermic transitions was also reported for fully hydrated DL-erythro C24:0-SM (Barenholz et al., 1976), D-erythro C24:0-SM (Cohen et al., 1984), and C24:0-SM derived from egg SM (McIntosh et al., 1992a) by deacylation-reacylation methods similar to those used here. For example, at a heating rate of 15°C/hr, McIntosh et al. (1992a) observed endothermic transitions at 39.6°C (H = 2.8 kcal/mol) and 46.2°C (H = 6.3 kcal/mol), in quite good agreement with transitions T_1 and T_2 described above. For C24:0-SM, we show that similar thermotropic behavior is observed at lower hydrations (see Fig. 1), but it is now clear that the high temperature shoulder associated with T_2 derives from the separate sharp transition T_3 at ~51°C observed at lower hydration; increasing overlap, particularly of T_2 and T_3, occurs as the transitions broaden at the higher hydrations. Also, it should be noted that anhydrous C24:0-SM exhibits a high melting transition; addition of 12 wt % water significantly reduces the transition temperature and leads to the formation of multiple gel phases. When hydration is increased further, all transitions (T_1, T_2, and T_3) decrease slightly in temperature; ΔH_{2+3} shows some hydration dependence, whereas ΔH_1 remains essentially constant (Fig. 2).

We have collected structural information on the phases present below T_1, between T_1 and T_2, and above T_3, but not between T_2 and T_3. X-ray diffraction data for C24:0-SM have been recorded and analyzed in terms of the hydration dependence of the structural parameters (d, d_1, S, and $d_{p\text{-}p}$) and the electron density profiles (Figs. 3 and 5). Below T_1, at 22°C, a gel phase is present at all hydration levels. This gel phase (Gel I) swells to a hydration limit of approximately 25 wt % water, corresponding to 15 mol H_2O/SM. The two wide-angle reflections at 1/4.2 $Å^{-1}$ and 1/4.0^{-1} (shoulder) are characteristic of a gel phase with pseudohexagonally packed hydrocarbon chains that are tilted with respect to the normal to the bilayer plane. The electron density profiles (Fig. 5 *a*) show that $d_{p\text{-}p}$ (49–50 Å) is essentially independent of hydration. In addition to the chain tilting of C24:0-SM in this Gel I phase suggested by the wide-angle diffraction data, partial chain interdigitation is predicted to occur at the bilayer center (see Fig. 6) based on the small value of $d_{p\text{-}p}$ and model building considerations (also, see McIntosh et al., 1992a). At low hydration, the calculated lipid thickness d_1 decreases with increasing hydration, but at hydration levels >24.5 wt % H_2O, the calculated lipid thickness d_1 is invariant (52.9 Å) and shows reasonable agreement (see Fig. 3) with $d_{p\text{-}p}$ (50 Å). The area

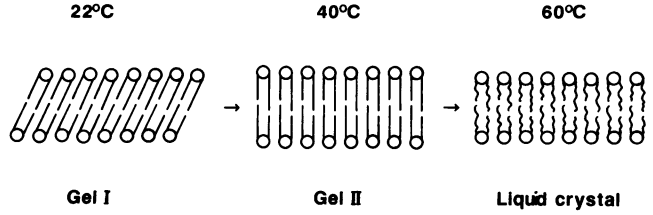

FIGURE 6 Schematic representation of the temperature-dependent bilayer structures formed by hydrated C24:0-SM.

per SM molecule (S) increases from 43.7 to a limiting value of 48.9 $Å^2$ and on the basis of the hydrocarbon chain area (20 $Å^2$/chain) again suggests that the chains are tilted with respect to the bilayer normal in this Gel I phase. In their study focusing exclusively on the low-temperature gel phase of C24:0-SM, McIntosh et al. (1992a) observed only a single, but broad, wide-angle reflection at 1/4.15 $Å^{-1}$ but concluded similarly that chain tilting occurs in this gel phase. Under different stress conditions, bilayer periodicities in the range 63.8–74.3 Å were observed (McIntosh et al., 1992a), in good agreement with our gravimetric values of 65.4–71.1 Å over the hydration range 9.1–25.4 wt % H_2O (see Fig. 3). McIntosh et al. (1992a,b) also derived electron density profiles for their equivalent of the Gel I phase; the profile with a $d_{p\text{-}p}$ of 51 Å is essentially identical to those shown in Fig. 5 (cf. $d_{p\text{-}p}$ = 49–50 Å). McIntosh et al. (1992a) also concluded that the chain packing mode consistent with all the diffraction data requires a juxtapositioning of the long C24 chain against a C18 chain from the opposite monolayer (see Fig. 6).

At 40°C, between T_1 and T_2, lamellar low-angle reflections, together with a single sharp wide-angle reflection at 1/4.2 $Å^{-1}$, are observed at all hydrations. This is indicative of a bilayer gel phase (Gel II) with hexagonal chain packing but with reduced chain tilt. Swelling is observed up to 29.5 wt % water; this corresponds to a hydration limit for Gel II of 19 mol H_2O/C24:0-SM, compared with 15 mol H_2O/mol SM for the Gel I phase. Over the hydration range 9.1–19.6 wt % H_2O, $d_{p\text{-}p}$ (= 52 Å) remains constant, but on further hydration $d_{p\text{-}p}$ increases to reach a limiting value, $d_{p\text{-}p}$ = 56 Å at hydration levels >29.5 wt % H_2O. It is noteworthy that a similar hydration dependence of $d_{p\text{-}p}$ was observed for the only gel phase of C18:0-SM (Maulik et al., 1991). These observations suggest that some decrease in chain tilt occurs with increasing hydration, although this argument is countered by the hydration dependence of d_l and S; d_l decreases continuously from 62.8 to 55.9 Å, and S increases from 42.0 to 47.0 $Å^2$ over the hydration range 9.1–29.5 wt % H_2O. However, the increment in $d_{p\text{-}p}$ and d_l from that observed in the Gel I phase plus the observation of a single wide-angle reflection at ~1/4.2 $Å^{-1}$ confirm that in the Gel II phase a decrease in chain tilt has occurred. Again, model building studies of the asymmetric C24:0-SM bilayer with untilted chains (bilayer thickness, 56 Å) are consistent with partial chain interdigitation across the bilayer center (see Fig. 6), a packing arrangement similar to that of Gel I. Thus, for C24:0-SM transition T_1 with a relatively small transition enthalpy (2.7–3.0 kcal/mol) involves the conversion of the chain-tilted, partially interdigitated bilayer gel phase (Gel I) to an untilted (or less tilted) bilayer gel phase (Gel II).

At 60°C (above T_3), the lamellar low-angle reflections and the diffuse wide-angle reflection at 1/4.6 $Å^{-1}$ observed at all hydrations is characteristic of the bilayer, liquid crystalline phase, L_α. Swelling is observed up to 29.5 wt % water; this corresponds to a hydration limit for the L_α phase of 19 mol H_2O/mol SM, a hydration limit identical to that of the Gel II phase. The bilayer thickness $d_{p\text{-}p}$ is essentially constant at 46 Å and in good agreement with that measured from single bilayer vesicles of C24:0-SM in the chain-melted state ($d_{p\text{-}p}$ = 47.5 Å; see Maulik et al., 1986a). The high degree of chain asymmetry of C24:0-SM would suggest some degree of chain interdigitation even in the L_α phase (see Fig. 6), as was observed in our previous x-ray scattering study of C24:0-SM (Maulik et al., 1986a). The observed $d_{p\text{-}p}$ is similar to the calculated d_l for hydrations >24.5 wt % H_2O. At lower hydrations, d_l decreases and S increases with increasing hydration, reaching limiting values of 48.5Å and 61.3 $Å^2$, respectively. This type of hydration-dependence of $d_{p\text{-}p}$, d_l, and S is characteristic of phospholipids in the liquid crystalline L_α phase. For example, the shorter chain C18:0-SM (Maulik et al., 1991) has smaller values of $d_{p\text{-}p}$ (41 Å) and d_l (45 Å) compared with C24:0-SM (see above), consistent with a predicted increase in bilayer thickness of the longer chain SM. Thus, the combination of transitions T_2 and T_3 (ΔH_{2+3} = 5.7 kcal/mol) converts the bilayer Gel II phase to the bilayer L_α phase.

Because of the hydrocarbon chain mismatch, C24:0-SM exhibits a more complex thermotropic behavior with multiple transitions (T_1, T_2, and T_3) compared with the "chain-matched" C16:0- and C18:0-SM, which exhibit a single reversible transition when studied under similar conditions. The DSC and x-ray diffraction studies reported here show that C24:0-SM has a well defined bilayer structure at all hydrations in the two gel phases (Gel I and Gel II) and in the liquid crystalline L_α phase. The x-ray diffraction data for C24:0 corresponding to full hydration show that the following structural changes occur at T_1: 1) the hydration limit and d_w increase, 2) the bilayer periodicity increases, 3) the lipid thickness, d_l and $d_{p\text{-}p}$, increases, and 4) the SM surface area decreases. In contrast, at T_{2+3} on chain melting, although the hydration limit is unchanged, 1) d_w decreases, 2) the bilayer periodicity decreases, 3) the lipid thickness, d_l and $d_{p\text{-}p}$, decreases, and 4) the area/SM increases. These structural changes have led to the following conclusions. 1) The low temperature transition (T_1) converts the tilted-chain, partially interdigitated bilayer gel phase (Gel I) to an untilted (or less tilted), interdigitated bilayer gel phase (Gel II); and (2) although we have been unable to define the structure of C24:0-SM present between transitions T_2 and T_3, a typical bilayer L_α phase is present above T_3. The combined enthalpy associated with T_2 and T_3 (5.7 kcal/mol) is consistent with a bilayer gel-bilayer liquid crystal transition associated with chain melting. The temperature-dependent structures of hydrated C24:0-CM are schematically represented in Fig. 6.

Because SM, PC, and cholesterol seem to coexist on both the outer monolayer of many plasma membranes and the surface monolayer of plasma lipoproteins, we have been interested in studying their interactions in mixed lipid systems, particularly in light of the suggestion that cholesterol has a stronger interaction with SM compared with PC. Although we have addressed such issues using both natural SM-PC (Untracht and Shipley, 1977) and synthetic SM-PC (Calhoun and Shipley, 1979b) and SM-PC-cholesterol (Calhoun and Shipley, 1979b) binary and ternary systems,

additional comparative studies using both "short" (C-16, C-18) and "long" (C-24) chain SMs are desirable.

We thank Dr. P.K. Sripada for synthesis of C24:0-SM, Dr. D. Atkinson for advice, and Ms. I. Miller for assistance in preparing this manuscript. This research was supported by Research Grant HL-26335 and Training Grant HL-07291 from the National Institutes of Health.

REFERENCES

Ahmad, T. Y., J. T. Sparrow, and J. D. Morrisett. (1985) Fluorine-, pyrene- and nitroxide-labeled sphingomyelin: semi-synthesis and thermotropic properties. *J. Lipid Res.* 26:1160–1165.

Barenholz, Y., J. Suurkuusk, D. Mountcastle, T. E. Thompson, and R. L. Biltonen. 1976. A calorimetric study of the thermotropic behavior of aqueous dispersions of natural and synthetic sphingomyelins. *Biochemistry.* 15:2441–2447.

Braganza, L. F., and D. L. Worcester. 1986. Hydrostatic pressure induces hydrocarbon chain interdigitation in single-component phospholipid bilayers. *Biochemistry.* 25:2591–2596.

Bruzik, K. S. 1988. Synthesis and spectral properties of chemically and stereochemically homogeneous sphingomyelin and its analogues. *J. Chem. Soc. Perkin Trans. I.* 423–431.

Bruzik, K. S., and M.-D. Tsai. 1987. A calorimetric study of the thermotropic behavior of pure sphingomyelin diastereomers. *Biochemistry.* 26:5346–5368.

Calhoun, W. I., and G. G. Shipley. 1979a. Fatty acid composition and thermal behavior of natural sphingomyelins. *Biochim. Biophys. Acta.* 555:436–441.

Calhoun, W. I., and G. G. Shipley. 1979b. Sphingomyelin-lecithin bilayers and their interaction with cholesterol. *Biochemistry.* 18:1717–1722.

Cohen, R., Y. Barenholz, S. Gatt, and A. Dagan. 1984. Preparation and characterization of well defined D-erythro sphingomyelins. *Chem. Phys. Lipids.* 35:371–384.

Dong, Z., and J. A. Butcher. 1993. An efficient route to N-palmitoyl-D-erythro-sphingomyelin and its ^{13}C-labeled derivatives. *Chem. Phys. Lipids.* 66:41–46.

Elliott, A. J. 1965. The use of toroidal reflecting surfaces in x-ray diffraction cameras. *J. Sci. Instrum.* 42:312–316.

Fishman, P. H., T. Pacuszka, and P. A. Orlandi. 1993. Gangliosides as receptors for bacterial enterotoxins. *Adv. Lipid Res.* 25:165–187.

Franks, A. 1958. Some developments and applications of microfocus x-ray diffraction techniques. *Br. J. Appl. Phys.* 9:349–352.

Haas, N. S., P. K. Sripada, and G. G. Shipley. 1990. Effect of chain-linkage on the structure of phosphatidylcholine bilayers: hydration studies of 1-hexadecyl 2-palmitoyl-*sn*-glycerol-3-phosphocholine. *Biophys. J.* 57:117–124.

Hakomori, S. I. 1981. Glycosphingolipids in cellular interaction, differentiaion and oncogenesis. *Annu. Rev. Biochem.* 50:733–764.

Hannun, Y. A. 1994. The sphingomyelin cycle and the second messenger function of ceramide. *J. Biol. Chem.* 269:3125–3128.

Hannun, Y. A., and L. M. Obeid. 1995. Ceramide: an intracellular signal for apoptosis. *Trends Biochem. Sci.* 20:73–77.

Hui, S. W., J. T. Mason, and C. Huang. 1984. Acyl chain interdigitation in saturated mixed-chain phosphatidycholine bilayer dispersions. *Biochemistry.* 23:5570–5577.

Janiak, M. J., D. M. Small, and G. G. Shipley. 1979. Temperature and compositional dependence of the structure of hydrated dimyristoyl lecithin. *J. Biol. Chem.* 254:6068–6078.

Kim, J. T., J. Mattai, and G. G. Shipley. 1987. Gel phase polymorphism in ether-linked dihexadecylphosphatidylcholine bilayers. *Biochemistry.* 26: 6592–6598.

King, G. I., and C. R. Worthington. 1971. Analytic continuation as a method of phase determination. *Phys. Lett.* 35A:259–260.

Levin, I. W., T. E. Thompson, Y. Barenholz, and C. Huang. 1985. Two types of hydrocarbon chain interdigitation in sphingomyelin bilayers. *Biochemistry.* 24:6282–6286.

Luzzati, V. 1968. X-ray diffraction studies of lipid-water systems. *In* Biological Membranes. D. Chapman, editor. Academic Press, London. 71–123.

Mattai, J., P. K. Sripada, and G. G. Shipley. 1987. Mixed-chain phosphatidylcholine bilayers: structure and properties. *Biochemistry.* 26: 3287–3297.

Maulik, P. R., D. Atkinson, and G. G. Shipley. 1986a. X-ray scattering of vesicles of N-acyl sphingomyelins: determination of bilayer thickness. *Biophys. J.* 50:1071–1077.

Maulik, P. R., P. K. Sripada, and G. G. Shipley. 1986b. The structure and properties of C16:0-SM and its interaction with cholesterol and dipalmitoylphosphatidylcholine. *Biophys. J.* 49:505*a*. (Abstr.)

Maulik, P. R., P. K. Sripada, and G. G. Shipley. 1991. Structure and thermotropic properties of hydrated N-stearoyl sphingomyelin bilayer membranes. *Biochim. Biophys. Acta.* 1062:211–219.

McDaniel, R. V., T. J. McIntosh, and S. A. Simon. 1983. Non-electrolyte substitution for water in phosphatidylcholine bilayers. *Biochim. Biophys. Acta.* 731:97–108.

McIntosh, T. J., and S. A. Simon. 1986. Hydration force and bilayer deformation: a reevaluation. *Biochemistry.* 25:4058–4066.

McIntosh, T. J., S. A. Simon, J. C. Ellington, Jr., and N. A. Porter. 1984. New structural model for mixed-chain phosphatidylcholine bilayers. *Biochemistry.* 23:4038–4044.

McIntosh, T. J., S. A. Simon, D. Needham, and C. Huang. 1992a. Structure and cohesive properties of sphingomyelin/cholesterol bilayers. *Biochemistry.* 31:2012–2020.

McIntosh, T. J., S. A. Simon, D. Needham, and C. Huang. 1992b. Interbilayer interactions between sphingomyelin and sphingomyelin/cholesterol bilayers. *Biochemistry.* 31:2020–2024.

Nagle, J. F., and D. A. Wilkinson. 1978. Lecithin bilayers. Density measurements and molecular interactions. *Biophys. J.* 23:159–175.

Ranck, J. L., T. Keira, and V. Luzzati. 1977. A novel packing of the hydrocarbon chains in lipids. The low temperature phases of dipalmitoyl phosphatidyl-glycerol. *Biochim. Biophys. Acta.* 488:432–441.

Ruocco, M. J., and G. G. Shipley. 1982. Characterization of the sub-transition of hydrated dipalmitoylphosphatidylcholine bilayers: kinetic, hydration and structural study. *Biochim. Biophys. Acta.* 691:309–320.

Ruocco, M. J., D. J. Siminovitch, and R. G. Griffin,. 1985. Comparative study of the gel phases of ether- and ester-linked phosphatidylcholines. *Biochemistry.* 24:2406–2411.

Serrallach, E. N., R. Dijkman, G. H. de Haas, and G. G. Shipley. 1983. Structure and thermotropic properties of 1,3-dipalmitoyl-glycero-2-phosphocholine. *J. Mol. Biol.* 170:155–174.

Shah, J., P. K. Sripada, and G. G. Shipley. 1990. Structure and properties of mixed-chain phosphatidylcholine bilayers. *Biochemistry.* 29:4254–4262.

Shannon, C. E. 1949. Communication in the presence of noise. *Proc. Inst. Radio. Eng. NY.* 38:10–21.

Shapiro, D. 1969. Chemistry of Sphingolipids. Hermann, Paris.

Shipley, G. G., L. S. Avecilla, and D. M. Small. 1974. Phase behavior and structure of aqueous dispersions of sphingomyelin. *J. Lipid Res.* 15: 124–131.

Simon, S. A., and T. J. McIntosh. 1984. Interdigitated hydrocarbon chain packing causes the biphasic transition behavior in lipid/alcohol suspensions. *Biochim. Biophys. Acta.* 773:169–172.

Sripada, P. K., P. R. Maulik, J. A. Hamilton, and G. G. Shipley. 1987. Partial synthesis and properties of a series of N-acyl sphingomyelins. *J. Lipid Res.* 28:710–718.

Tardieu, A., V. Luzzati, and F. C. Reman. 1973. Structure and polymorphism of the hydrocarbon chains of lipids: a study of lecithin-water phases. *J. Mol. Biol.* 75:711–733.

Torbet, J., and M. H. F. Wilkins. 1976. X-ray diffraction study of lecithin bilayers. *J. Theor. Biol.* 62:447–458.

Untracht, S. H., and G. G. Shipley. 1977. Molecular interactions between lecithin and sphingomyelin: temperature-and composition-dependent phase separation. *J. Biol. Chem.* 252:4449–4457.

Wiener, M. C., R. M. Suter, and J. F. Nagle. 1989. Structure of the fully hydrated gel phase of dipalmitoylphosphatidylcholine. *Biophys. J.* 55: 315–325.

Worthington, C. R., and A. E. Blaurock. 1969. A structural analysis of nerve myelin. *Biophys. J.* 9:970–990.